Optimal Barrier Locations for The Best Performances in Recycled Membrane Extractors (2/3)

回流型薄膜萃取器之最佳回流隔板位置及效率之提高(2/3)

計畫編號: NSC 92-2214-E-032-001

執行期限: 92/08/01~ 93/07/31

(期中報告)

Ho-Ming. Yeh (葉和明)
Department of Chemical and Matirials Engineering, Tamkang University, Tamsui,
Taiwan 251

淡江大學化學工程與材料工程學系

Abstract

The influence of recycle-barrier location on membrane extraction through a parallel-flow rectangular module with internal reflux has been investigated. The recycle barrier is placed in the raffinate phase to divide the flow channel into an operating subchannel and a reflux subchannel and thus, there are concurrent flow in one subchannel and countercurrent flow in another subchannel. It was found that larger part of mass-transfer area for countercurrent-flow channel, as well as smaller part of mass-transfer area for concurrent-flow channel, is beneficial to total mass-transfer rate. It was also noted that with the recycle-barrier location moving from the centerline of the raffinate phase to create larger mass-transfer area for countercurrent-flow channel, as well as to decrease mass-transfer area for concurrent-flow channel, the same performance can be achieved with reducing the reflux ratio.

Keyword: Membrane extraction; Reflux; Recycle-barrier location; Parallel flow

---

*Corresponding author. Tel. : +886-02-9180149; fax: +886-02-26203887
E-mail address: hmyeh@mail.tku.edu.tw (H. M. Yeh)

1. Introduction

Membrane extraction is carried out in a microporous membrane device, in which the membrane is generally contacted with two immiscible fluids at two sides (phases *a* and *b*). However, if these two fluids are miscible, then the pores of the membrane is filled with another fluid (phase *c*) which is immiscible with these two fluids. The solute is extracted from phase *a* to phase *c* and then to phase *b*, or vice versa. This new technique overcomes the limitations of conventional liquid extraction, such as flooding, intimate mixing, limitations on independent phases flow rate variations, requirement of density difference and inability to handle particulates (Lo & Baird, 1980).

Application of the external or internal reflux to the design and operation of a mass- or heat- transfer equipment can effectively enhance the effect on mass or heat transfer, leading to improved performance (Garcia-Calvo, Rodriguez, Prados & Klein, 1998; Goto & Gaspillo, 1992; Ho, Yeh & Sheu, 1988; Kikuchi, Takahashi, Takeda & Sugawara, 1999; Korpijarvi, Oinas & Reunanen, 1998; Santacesaria, Di Serio & Iengo, 1999; Stenas, Clark & Lazarova, 1999; Tsai & Yeh, 1985; Yeh, Cheng & Tsai, 1986; Yeh, Tsai & Chiang, 1987; Yeh , Tsai & Lin, 1986). Recently, the recycle effect on solvent extraction in microporous-membrane modules has been studied both theoretically and experimentally (Yeh & Chen, 2001; Yeh, Peng & Chen, 1999). For solvent extraction through a membrane modules, the recycle effect is favorable for the system with higher distribution coefficients where the liquid-phase mass-transfer resistances are more extremely predominant. It is the purpose of this work to investigate the influence of recycle-barrier location in the raffinate phase on solvent extraction through a double-pass parallel-plate membrane module with internal reflux.

2. Theory

Being a parallel-flow device, there are two different flow patterns for operation. Fig. 1 shows the system with concurrent flow first and then followed by countercurrent flow. On the other hand, Fig. 2 illustrates the system with countercurrent flow first and then followed by concurrent flow.

2.1. Concurrent-flow operation with countercurrent-flow reflux

As shown in Fig. 1, an impermeable plate with negligible thickness is placed in vertical to the upper plate and the membrane sheet, at a certain line of channel *a* (phase *a*) to divide the raffinate phase into two subchannels (subchannels a_1 and a_2) of widths Δw and $(1-\Delta)\,w$, respectively, and that a pump is installed for internal reflux. Thus, in the raffinate phase (phase *a*), the inlet fluid of volume rate Q_a mixed with the outlet reflux fluid of volume rate RQ_a, flows steadily as well as concurrently and countercurrently within subchannels a_1 and a_2, respectively. The extract phase (phase *b*) with inlet volume rate Q_b flows steadily through channel *b*.

Referring to Fig. 1, the mass balance over the right-hand section of the membrane extractor operated, with reflux ratio *R*, is

$$Q_b(C_{b,e} - C_b) = (1+R)Q_a C_{a,1} - RQ_a C_{a,2} - Q_a C_{a,e} \tag{1}$$

or

$$C_b = C_{b,e} - \left(\frac{Q_a}{Q_b}\right)[(1+R)C_{a,1} - RC_{a,2} - C_{a,e}] \tag{2}$$

Considering the mass transfer on subchannels a_1 and a_2 over the length *dx*

$$-(1+R)Q_a dC_{a,1} = K_1 \Delta w (H_{ac} C_{a,1} - H_{bc} C_b)dx \tag{3}$$

$$RQ_a dC_{a,2} = K_2(1-\Delta)w(H_{ac}C_{a,2} - H_{bc}C_b)dx \tag{4}$$

where K_1 and K_2 are the overall mass-transfer coefficients in subchannels a_1 and a_2, respectively, while H_{ac} and H_{bc} are the distribution coefficients between two different phases, as defined by

$$H_{ac} = \frac{\text{solute concentration in phase c}}{\text{solute concentration in phase a}} \tag{5}$$

Substituting the value of C_b from Eq. (2) into Eqs. (3) and (4), one obtains

$$\frac{dC_{a,1}}{dx} + \zeta\, C_{a,1} + \zeta^{\circ} C_{a,2} = \varsigma C_{b,e} + \varsigma^{\circ} C_{a,e} \tag{6}$$

$$\frac{dC_{a,2}}{dx} + \varpi\, C_{a,2} + \varpi^{\circ} C_{a,1} = \xi C_{b,e} + \xi^{\circ} C_{a,e} \tag{7}$$

where

$$\zeta = K_1 \Delta w[\frac{H_{ac}}{(1+R)Q_a} + \frac{H_{bc}}{Q_b}] \tag{8}$$

$$\zeta^{\circ} = -\frac{K_1 \Delta w R}{(1+R)}(\frac{H_{bc}}{Q_b}) \tag{9}$$

$$\varsigma = \frac{K_1 \Delta w}{(1+R)}(\frac{H_{bc}}{Q_a}) \tag{10}$$

$$\varsigma^{\circ} = \frac{K_1 \Delta w}{(1+R)}(\frac{H_{bc}}{Q_b}) \tag{11}$$

$$\varpi = -K_2(1-\Delta)w(\frac{H_{ac}}{RQ_a} - \frac{H_{bc}}{Q_b}) \tag{12}$$

$$\varpi^{\circ} = -\frac{K_2(1-\Delta)w(1+R)}{R}(\frac{H_{bc}}{Q_b}) \tag{13}$$

$$\xi = -\frac{K_2(1-\Delta)w}{R}(\frac{H_{bc}}{Q_a}) \tag{14}$$

$$\xi^{\circ} = -\frac{K_2(1-\Delta)w}{R}(\frac{H_{bc}}{Q_b}) \tag{15}$$

Eqs. (6) and (7) can be solved simultaneously for solute concentrations, $C_{a,1}$ and $C_{a,2}$, in subchannels a_1 and a_2 with the following boundary conditions:

at $x=L$, $C_{a,1} = C_{a,2} = C_{a,e}$ (16)

The general solutions of Eqs.(6) and (7) are

$$C_{a,1} = \alpha e^{\lambda_a x} + \beta e^{\lambda_b x} + nC_{b,e} + mC_{a,e} \tag{17}$$

$$C_{a,2} = \frac{1}{\zeta^0}[-(\lambda_a + \zeta)\alpha e^{\lambda_a x} - (\lambda_b + \zeta)\beta e^{\lambda_b x} + (\varsigma - \zeta n)C_{b,e} + (\varsigma^0 - \zeta m)C_{a,e}] \tag{18}$$

where

$$\lambda_a = \frac{-(\zeta + \varpi) + \sqrt{(\zeta - \varpi)^2 + 4\zeta^{\circ}\varpi^{\circ}}}{2} \tag{19}$$

$$\lambda_b = \frac{-(\zeta + \varpi) - \sqrt{(\zeta - \varpi)^2 + 4\zeta^{\circ}\varpi^{\circ}}}{2} \tag{20}$$

$$n = \frac{\varpi\varsigma - \zeta^{\circ}\xi}{\zeta\varpi - \zeta^{\circ}\varpi^{\circ}} \tag{21}$$

$$m = \frac{\varpi\varsigma^{\circ} - \zeta^{\circ}\xi^{\circ}}{\zeta\varpi - \zeta^{\circ}\varpi^{\circ}} \tag{22}$$

while α and β are the integration constants which are determined by Eq. (16) as

$$\alpha = \frac{e^{-\lambda_a L}}{(\lambda_a - \lambda_b)}[(n\lambda_b + \varsigma)C_{b,e} + (m\lambda_b + \varsigma^0 - \lambda_b - \zeta - \zeta^0)C_{a,e}] \tag{23}$$

$$\beta = \frac{e^{-\lambda_b L}}{(\lambda_a - \lambda_b)}[-(n\lambda_a + \varsigma)C_{b,e} - (m\lambda_a + \varsigma^0 - \lambda_a - \zeta - \zeta^0)C_{a,e}] \qquad (24)$$

If mixed inlet concentration $C^o_{a,i}$ and the outlet reflux concentration $C'_{a,e}$ are introduced into Eqs. (17) and (18), respectively, i.e.

at $x = 0$, $C_{a,1} = C^o_{a,i}$ (25)

at $x = 0$, $C_{a,2} = C'_{a,e}$ (26)

one obtains, with the substitution of Eqs. (23) and (24)

$$C^\circ_{a,i} = AC_{b,e} + BC_{a,e} \qquad (27)$$

$$C'_{a,e} = EC_{b,e} + FC_{a,e} \qquad (28)$$

where

$$A = \frac{(n\lambda_b + \varsigma)e^{-\lambda_a L} - (n\lambda_a + \varsigma)e^{-\lambda_b L}}{(\lambda_a - \lambda_b)} + n \qquad (29)$$

$$B = \frac{(m\lambda_b + \varsigma^\circ - \lambda_b - \zeta - \zeta^\circ)e^{-\lambda_a L}}{(\lambda_a - \lambda_b)}$$

$$- \frac{(m\lambda_a + \varsigma^\circ - \lambda_a - \zeta - \zeta^\circ)e^{-\lambda_b L}}{(\lambda_a - \lambda_b)} + m \qquad (30)$$

$$E = \frac{1}{\zeta^\circ}[\frac{(\lambda_a + \zeta)(n\lambda_b + \varsigma)e^{-\lambda_a L}}{(\lambda_b - \lambda_a)}$$

$$- \frac{(\lambda_b + \zeta)(n\lambda_a + \varsigma)e^{-\lambda_b L}}{(\lambda_b - \lambda_a)} + (\varsigma - \zeta n)] \qquad (31)$$

$$F = \frac{1}{\zeta^\circ}[\frac{(\lambda_a + \zeta)(m\lambda_b + \varsigma^\circ - \lambda_b - \zeta - \zeta^\circ)e^{-\lambda_a L}}{(\lambda_b - \lambda_a)}$$

$$- \frac{(\lambda_b + \zeta)(m\lambda_a + \varsigma^\circ - \lambda_a - \zeta - \zeta^\circ)e^{-\lambda_b L}}{(\lambda_b - \lambda_a)} + (\varsigma^\circ - \zeta m)] \qquad (32)$$

Inspection of Eqs. (27) and (28) shows that the outlet concentrations, $C'_{a,e}$, $C_{a,e}$ and $C_{b,e}$, as well as the mixed inlet concentration $C^{o}_{a,i}$, are not specified a priori. Mathematically, two more relations are needed for determination of these values. For this purpose, two mass balances for solutes at the inlet of phase *a* and through the whole module are readily obtained, respectively, as

$$C_{a,i} + RC'_{a,e} = (1+R)C^{\circ}_{a,i} \tag{33}$$

$$C_{b,e} = C_{b,i} + (\frac{Q_a}{Q_b})(C_{a,i} - C_{a,e}) \tag{34}$$

By solving Eqs.(27), (28) and (33) simultaneously,one has

$$C^{\circ}_{a,i} = [\frac{R(BE-AF)}{B+BR-FR}]C_{b,e} + (\frac{B}{B+BR-FR})C_{a,i} \tag{35}$$

$$C_{a,e} = [\frac{ER-A(1+R)}{B+BR-FR}]C_{b,e} + (\frac{1}{B+BR-FR})C_{a,i} \tag{36}$$

Substituting Eq.(34) into Eq.(36), we obtain the outlet concentration from phase a

$$C_{a,e} = \{\frac{Q_a[ER-A(1+R)]+Q_b}{Q_b(B+BR-FR)+Q_a[ER-A(1+R)]}\}C_{a,i}$$

$$+\{\frac{Q_b[ER-A(1+R)]}{Q_b(B+BR-FR)+Q_a[ER-A(1+R)]}\}C_{b,i} \tag{37}$$

Substitution of Eq.(37) into Eq.(34) gives the expression for calculation of the outlet concentration from phase b, $C_{b,e}$.

2.2. Countercurrent-flow operation with concurrent-flow reflux

Figure 2, shows a schematic diagram of the rectangular system of countercurrent-flow membrane extraction with concurrent-flow reflux. Referring to Fig. 2, the mass balance over the right-hand section of the membrane extractor operated, with reflux ratio R, is

$$Q_b(C_b - C_{b,i}) = (1+R)Q_a C_{a,1} - RQ_a C_{a,2} - Q_a C_{a,e} \qquad (38)$$

or

$$C_b = C_{b,i} + (\frac{Q_a}{Q_b})\left[(1+R)\ Q_a C_{a,1} - RQ_a C_{a,2} - C_{a,e}\ \right] \qquad (39)$$

Considering the mass transfer on subchannels a_1 and a_2 over the length dx

$$-(1+R)Q_a dC_{a,1} = K_1 \Delta w(H_{ac}C_{a,1} - H_{bc}C_b)dx \qquad (40)$$

$$RQ_a dC_{a,2} = K_2(1\text{-}\Delta)\mathrm{w}(H_{ac}C_{a,2} - H_{bc}C_b)dx \qquad (41)$$

Substituting the value of C_b from Eq. (39) into Eqs. (40) and (41), one obtains

$$\frac{dC_{a,1}}{dx} + \zeta' C_{a,1} - \zeta^0 C_{a,2} = \varsigma C_{b,i} - \varsigma^0 C_{a,e} \qquad (42)$$

$$\frac{dC_{a,2}}{dx} + \varpi' C_{a,2} - \varpi^\circ C_{a,1} = \xi C_{b,i} - \xi^\circ C_{a,e} \qquad (43)$$

where

$$\zeta' = K_1 \Delta w[\frac{H_{ac}}{(1+R)Q_a} - \frac{H_{bc}}{Q_b}] \qquad (44)$$

$$\varpi' = -K_2(1-\Delta)w(\frac{H_{ac}}{RQ_a} + \frac{H_{bc}}{Q_b}) \qquad (45)$$

in which $C_{a,e}$ can be solved from Eqs.(42) and (43) by following the same mathematical procedure performed in section 2.1. with the use of the additional mass balances, Eqs.(33) and (34), as well as the appropriate boundary conditions, Eqs.(16), (25) and (26).

The result is

$$C_{a,e} = [\frac{E'R - A'(1+R)}{B' + B'R - F'R}]C_{b,i} + (\frac{1}{B' + B'R - F'R})C_{a,i} \tag{46}$$

where

$$A' = \frac{(n'\lambda'_b + \varsigma)e^{-\lambda'_a L} - (n'\lambda'_a + \varsigma)e^{-\lambda'_b L}}{(\lambda'_a - \lambda'_b)} + n' \tag{47}$$

$$B' = \frac{(m'\lambda'_b + \varsigma^{\circ} - \lambda'_b - \zeta' - \zeta^{\circ})e^{-\lambda'_a L}}{(\lambda'_a - \lambda'_b)} - \frac{(m'\lambda'_a + \varsigma^{\circ} - \lambda'_a - \zeta' - \zeta^{\circ})e^{-\lambda'_b L}}{(\lambda'_a - \lambda'_b)} + m' \tag{48}$$

$$E' = \frac{1}{\zeta^{\circ}}[\frac{(\lambda'_a + \zeta')(n'\lambda'_b + \varsigma)e^{-\lambda'_a L}}{(\lambda'_b - \lambda'_a)} - \frac{(\lambda'_b + \zeta')(n'\lambda'_a + \varsigma)e^{-\lambda'_b L}}{(\lambda'_b - \lambda'_a)} + (\varsigma - \zeta' n')] \tag{49}$$

$$F' = \frac{1}{\zeta^{\circ}}[\frac{(\lambda'_a + \zeta')(m'\lambda'_b + \varsigma^{\circ} - \lambda'_b - \zeta' - \zeta^{\circ})e^{-\lambda'_a L}}{(\lambda'_b - \lambda'_a)}$$

$$- \frac{(\lambda'_b + \zeta')(m'\lambda'_a + \varsigma^{\circ} - \lambda'_a - \zeta' - \zeta^{\circ})e^{-\lambda'_b L}}{(\lambda'_b - \lambda'_a)} + (\varsigma^{\circ} - \zeta' m')] \tag{50}$$

$$\lambda'_a = \frac{-(\zeta' + \varpi') + \sqrt{(\zeta' - \varpi')^2 + 4\zeta^{\circ}\varpi^{\circ}}}{2} \tag{51}$$

$$\lambda'_b = \frac{-(\zeta' + \varpi') - \sqrt{(\zeta' - \varpi')^2 + 4\zeta^{\circ}\varpi^{\circ}}}{2} \tag{52}$$

$$n' = \frac{\varpi'\varsigma - \zeta^{\circ}\xi}{\zeta'\varpi' - \zeta^{\circ}\varpi^{\circ}} \tag{53}$$

$$m' = \frac{-\varpi'\varsigma^{\circ} - \zeta^{\circ}\xi^{\circ}}{\zeta'\varpi' - \zeta^{\circ}\varpi^{\circ}} \tag{54}$$

2. 3. Mass-transfer rate

Once the outlet concentrations, $C_{a,e}$ and $C_{b,e}$, obtained from Eqs.(37) and (34) and from Eqs.(46) and (34), respectively, for councurrent-flow and countercurrent-flow operations, the total mass-transfer rates will be determined by Eq. (55).

$$W = Q_a(C_{a,i} - C_{a,e}) = Q_b(C_{b,e} - C_{b,i}) \tag{55}$$

3. Numerical Example

For the purpose of illustration, let us employ the experimental data of previous work (Yeh, Peng & Chen, 1999). Experiments were carried out with the use of a membrane sheet (l=w=0.165m) made of microporous polypropylene (Gelman Sciences, average pore size=0.2 μm, porosity=70% and thickness=178μm) as a permeable barrier to extract acetic acid(reagent ACS grade, Fisher) from aqueous solution by methyl isobutyl ketone (MIBK, regent grade, Fisher). The membrane sheet was inserted in parallel between two parallel plates of stainless steel, with same distance from them to divide the conduit into two channels(channels a and b, or phases a and b) of same height ($h = 1.9 \times 10^{-3}\, m$). Since microporous polypropylene is hydropholic membranes, the organic solution (solute: acetic; solvent: MIBK) wets the membrane, and thus $H_{bc} = 1$ and $H_{ac} = 0.524$ at $25\,^{o}C$ (Yeh & Huang, 1995).

The following correlation equations for estimating the average values of overall mass-transfer coefficient applicable to such small velocity ranges (Q_a=0.188~0.847 cm^3/s, Q_b=0.25cm^3/s) were obtained (Yeh, Peng & Chen, 1999) as :

For $C_{a,i} = 5\times10^{-4}\, mole/cm^3$,

$K_i \times 10^4 (cm/s) = 3.865 + 1.484 v_{a,i} (cm/s)$ (concurrent flow; i=1 for Section 2.1. and i=2 for Section 2.2.) (56)

$K_i \times 10^4 (cm/s) = 5.012 + 0.718 v_{a,i} (cm/s)$ (countercurrent flow; i=1 for Section 2.2. and i=2 for Section 2.1.) (57)

For $C_{a,i} = 2.02\times10^{-3} \quad mole/cm^3$,

$K_i \times 10^4 (cm/s) = 2.152 + 0.846 v_{a,i} (cm/s)$ (concurrent flow; i=1 for Section 2.1. and i=2 for Section 2.2.) (58)

$K_i \times 10^4 (cm/s) = 3.177 + 0.733 v_{a,i} (cm/s)$ (countercurrent flow; i=1 for Section 2.2. and i=2 for Section 2.1.) (59)

in which the fluid velocities, $v_{a,1}$ and $v_{a,2}$ (cm/s), in phase a is related with the reflux ratio R as

$$v_{a,1} = \frac{Q_a(1+R)}{h\Delta w} \tag{60}$$

$$v_{a,2} = \frac{Q_a R}{h(1-\Delta)w} \tag{61}$$

4. Results and discussion

4.1. *Effect of Δ on performance*

It is seen in Fig.3 that for the device of concurrent-flow operation with countercurrent-flow reflux, mass-transfer rate increases when the width fraction (Δ) of concurrent-flow channel (subchannel a_1) decreases, or that ($1-\Delta$) of countercurrent-flow channel (subchannel a_2) increases. On the other hand, Fig. 4 shows that for the device of countercurrent-flow operation with concurrent-flow reflux, mass-transfer rate increases with the width fraction (Δ) of countercurrent-flow channel (subchannel a_1) increases, or that ($1-\Delta$) of concurrent-flow channel (subchannel a_2) decreases. These are because that for mass transfer, the countercurrent-flow effect is more effective than the concurrent-flow effect, and that larger part of mass-transfer area for countercurrent-flow channel, as well as smaller part of mass-transfer area for concurrent-flow channel, is beneficial to total mass-transfer rate. Further, the performance of higher inlet concentration overcomes the performance of lower inlet concentration, as comparing Fig. (3a) with Fig. (3b), as well as Fig. 4(a) with Fig. 4(b).

It is better to illustrate the improvement of performance *I* based on that obtained with the recycle barrier located at the centerline (Δ=0.5) of the raffinate phase

$$I = \frac{W - W_{\Delta=0.5}}{W_{\Delta=0.5}} \tag{62}$$

The results are listed in Tables 1 and 2 for two types of operation. It is seen in these tables that *I* obtained in the second type by increasing the mass-transfer area for countercurrent-flow operation (Δ>0.5), as shown in Fig. 2(a), overcomes that obtained in the first type by increasing the mass-transfer area for countercurrent-flow reflux (Δ<0.5), as shown in Fig. 1(a). This is because that the flow rates for countercurrent-flow operation, $(1+R)Q_a$, is larger than that for countercurrent-flow reflux, RQ_a, leading to further improved mass-transfer rate, especially for small Q_a and R.

4.2. *Effect of Δ on reduction of R*

Figures 5 and 7 illustrate the comparision of the performance obtained for R=1 and Δdiffering from 0.5 with that obtained for Δ=0.5 and R larger than unity, under low flow-rate operations in raffinate phase. It is seen in these figures that with the recycle-barrier location moving gradually from the centerline ($\Delta \rightarrow 0$ for concurrent-flow operation, and $\Delta \rightarrow 1$ for countercurrent-flow operation, of the systems described in Section 2.1. and Section 2.2., respectively), the number of reflux ratio R reguired may be gradually reducing for obtaining the same performance. As we can see in Fig. 5(b) that the mass-transfer rate W for Δ=0.1 and R=1 is larger than that for Δ=0.5 and R=2 while in Fig.7(b), W for Δ=0.9 and R=1 is larger than that for Δ=0.5 and R=3. Same results for reducing reflux ratio by increasing the mass-transfer area of countercurrent-flow channel to achieve the same performance are also shown in Figs.6 and 8.

Some numerical values of predicting result for W and I are listed in Tables 1 and 2, which give the same results described above.

4.3. *Effect of Δ on hydraulic dissipated loss*

In present study, an impermeable barrier with negligible thickness is placed in vertical to the upper plate and membrane sheet, at an adjustable location of channel a (phase a) to divide the channel into two subchannels

(subchannels a_1 and a_2) of widths Δw and $(1-\Delta)\, w$ for internal reflux. Though considerable improvement in mass transfer can be obtained by adjusting the location of barrier plate, and/or operating with recycle, the hydraulic dissipated energy due to the friction loss of fluid flow should be discussed.

The hydraulic dissipated power in a parallel-plate channel may be estimated by

$$H = (\textit{fluid density} \times \textit{volumn flow rate}) \times \frac{\Delta P}{\textit{fluid density}}$$

$$= (\textit{volume flow rate}) \times \Delta P \qquad (63)$$

If laminar flow in the flow channels is assumed, the pressure drop through the flow channel is (Bird, Stewart & Lightfoot, 1971)

$$\Delta P = \frac{12\mu\, l \times (\textit{volumn flow rate})}{h^2 \times (\textit{cross-section area of channel})} \qquad (64)$$

Since the total hydraulic dissipated energy includes those in subchannel a_1, subchannel a_2 and channel b, we have

$$H = H_{a,1} + H_{a,2} + H_b$$

$$= \left[Q_a(1+R) \times \frac{12\mu_a l\, Q_a(1+R)}{h^3 \Delta w} \right] + \left[Q_a R \times \frac{12\mu_a l\, Q_a R}{h^3 (1-\Delta) w} \right] + \left[Q_b \times \frac{12\mu_b l\, Q_b}{h^3 w} \right]$$

$$= \frac{12l}{h^3 w} \left[\frac{\mu_a Q_a{}^2 [(1+R)^2 - (1+2R)\Delta}{\Delta(1-\Delta)} + \mu_b Q_b{}^2 \right] \qquad (65)$$

The total hydraulic dissipated energies H for various operating conditions were calculated by Eq. (65) with $l = w = 16.5cm$, $h = 0.19cm$, $\mu_a = 1 \times 10^{-2} g/cm \cdot s$ and $\mu_b = 0.58 \times 10^{-2} g/cm \cdot s$. Some of the results of H are also listed in Table 1. It is shown in this table that H increases when the recycle barrier goes far from the centerline (Δ=0.5), as well as R and/or Q_a increases. However, the hydraulic dissipated energy is very small even for the system of extremely large or small Δ, as well as for that of large R and Q_a. For instance, $H = 9.1\times 10^{-7}\,hp$ for Δ=0.9, R=9 and Q_a=0.8 cm^3/s.

5. Conclusion

The performance of membrane extraction through rectangular mass exchangers with internal reflux has been analyzed under cocurrent-flow and countercurrent-flow operations. The ordinary differential equations for solute concentration distributions in the raffinate and extract phases were derived based on mass balances with the assumptions of uniform concentrations and velocities over cross-sections of flow channels. The outlet concentration were solved simultaneously from the governing equations with the use of appropriate boundary conditions. Once the outlet concentrations were obtained, the overall mass-transfer rates W for two types of flow were predicted. The results are plotted in Figs 3-8 and listed in Tables 1 and 2. It is found that W increases with Q_a, $C_{a,i}$ and R, as well as with Δ of values approaching zero for concurrent-flow operation and approaching unity for countercurrent-flow operation. It is also noted that the order of mass transfer rate in two types of mass exchanger is: *countercurrent-flow operation with concurrent-flow reflux* $>$ *concurrent-flow operation with countercurrent-flow reflux.*

The effect of recycle-barrier location on performance was also further investigated. It was found that larger part of mass-transfer area for countercurrent-flow channel as well as smaller part of mass-transfer area for concurrent-flow channel, is benifical to total mass-transfer rate, and that with the recycle-barrier location moving from the centerline to create larger mass-transfer area for countercurrent-flow channel, the reflux ratio can be reduced for achieving the same performance. However, the hydraulic dissipated energies though are extremely small, they increase rapidly with reflux ratio as well as when the recycle barrier goes far from the centerline ($\Delta = 0.5$), as shown in Tables 1 and 2. Therefore, the increase of operating cost due to the friction loss of fluid flow should be also taken into consideration when design.

Notation

A, B, E, F	Constant defined by Eqs. (29)-(32)
A', B', C', F'	Constant defined by Eqs. (45)-(48)
C_a, C_b	Bulk solute concentrations in raffinate phase (phase a), and in extract phase (phase b), $mole/cm^3$
$C_{a,e}, C_{b,e}$	Outlet solute concentrations in phase a. and in phase b , $mole/cm^3$
$C'_{a,e}$	Outlet concentration in subchannel a_2, $mole/cm^3$
$C_{a,i}, C_{b,i}$	Inlet solute concentration in phase a, in phase b , $mole/cm^3$
$C^o_{a,i}$	Mixed inlet concentration in phase a , $mole/cm^3$
C_{a1}, C_{a2}	Bulk solute concentrations in subchannel a_1 , in

	subchannel a_2 of phase a $, mole / cm^3$
H	Hydraulic dissipated power, hp
H_{ij}	Distribution coefficient between phase i and phase j
h	Half height of parallel channel, or distance between flat plate and membrane sheet ,cm
K_i	Average overall mass-transfer coefficient, i=1 and 2,cm/s
L	The length of membrane sheet ,cm
$n, \ n'$	Constant defined by Eq. (21) and Eq.(53), respectively
$m, \ m'$	Constant defined by Eq. (22) and Eq.(54), respectively
ΔP	Pressure drop in flow channel, N/cm^2
Q_a, Q_b	Inlet volume rates in phase a, in phase b $, cm^3 / s$
R	Reflux ratio, reverse volume rate RQ_a divided by inlet volume rate Q_a
S	Overall mass-transfer area of a flat-plate membrane module Lw, cm^2
$v_{a,1}, v_{a,2}$	Fluid velocity in subchannel a_1 , in subchannel a_2 ,cm/s
v_b	Fluid velocity in phase b ,cm/s
w	Width of membrane sheet ,cm
x	Axis along the flow direction
I	Improvement in performance defined by Eq. (62)

Greek letters

α	Constant defined by Eq. (23)
β	Constant defined by Eq. (24)
Δ	Width fraction of subchannel a_1, $\Delta w / w$
ζ, ζ^0, ζ'	Constant defined by Eqs. (8), (9) and (49), respectively
ς, ς^0	Constant defined by Eqs. (10) and (11), respectively
$\varpi, \varpi^0, \varpi'$	Constant defined by Eqs. (12), (13) and (50), respectively
ξ, ξ^0	Constant defined by Eqs. (14) and (15), respectively
λ_a, λ_b	Constant defined by Eqs. (19) and (20), respectively
λ'_a, λ'_b	Constant defined by Eqs. (51) and (52), respectively
μ_a, μ_b	Fluid viscosities of phase a and phase b, respectively, $g / cm \cdot s$

Acknowledgements

We wish to express our thanks to the National Science Council of R. O. C. for financial aid under Grand No. NSC-91-2214-E-032-001 and Grand No. NSC-92-2214-E-032-001.

References

Bird, R.B., Stewart, W.E. & Lightfoot, E.N. (1971). Transport Phenomena, p.62, New York: Wiley.

Garcia-Calvo, E., Rodriguez, A., Prados, A., & Klein, J. (1998). Fluid dynamic model for three-phase airlift reactors. *Chemical Engineering Science*, *54*, 2359.

Goto, S., & Gaspillo, P. D. (1992). Effect of static mixer on mass transfer in draft tube bubble column and in external loop cilomn. *Chemical Engineering Science*, *47*, 3533.

Ho, C. D., Yeh, H. M., & Sheu, W. S. (1988). The analytical studies of heat and mass transfer through a parallel-plate channel with recycle. *International Journal of Heat Mass Transf*er, *41*, 2589.

Kikuchi, K. I., Takahashi, H., Takeda, Y., & Sugawara, F. (1999). Hydrodynamic behavior of single particles in a draft-tube bubble column. *Can. J. Chem. Eng.*, *77*, 573.

Korpijarvi, J., Oinas, P., & Reunanen, J. (1998). Hydrodynamics and mass transfer in airlift reactor. *Chemical Engineering Science*, *54*, 2255.

Lo, T. C., & Baird, M. H. I. (1980). Liquid-Liquid Extraction. In M. Grayson, *Kirktothmer Encyclopedia of Chemical Technology*. Vol. 9, (3rd ed.). New York: Wiley.

Santacesaria, E., Di Serio, M., & Iengo, P. (1999). Mass transfer and kinetics in ethoxylation spray tower loop reactors. *Chemical Engineering Science*, *54*, 1499.

Stenas, M., Clark, M., & Lazarova, V. (1999). Holdup and liquid circulation velocity in a rectangular air-lift bioreactor. *Ind. Eng. Chem. Res*. *38*, 944.

Tsai, S. W., & Yeh, H. M. (1985) A study of the separation efficiency in horizontal thermal diffusion columns with external refluxes. *The Canadian Journal of Chemical Eng*ineering, *63*, 406.

Yeh, H. M., & Chen, C. H. (2001). Recycle effects on solvent extraction through concurrent-flow parallel-plate membrane modules. *Journal of Membrane Science*, *190*, 35.

Yeh, H. M., Cheng, T. W., & Tsai, S. W. (1986). A study of the gratez problem in concentric-tube continuous-contact countercurrent separation processes with recycles at both ends. *Separation Science Technology, 21*, 403.

Yeh, H. M., & Huang, C. M. (1995). Solvent extraction in multipass parallel-flow mass exchangers of microporous hollow-fiber modules. *Journal of Membrane Science, 103,* 135.

Yeh, H. M., Peng, Y. Y., & Chen, Y. K. (1999). Solvent extraction through a double-pass parallel-plate membrane channel with recycle. *Journal of Membrane Science*, *163*, 177.

Yeh, H. M., Tsai, S. W., & Chiang, C. L. (1987). Recycle effects on heat and mass transfer through a parallel-plate channel. *AIChE Journal*, *33*, 1743.

Yeh, H. M., Tsai, S. W., & Lin, C. S. (1986). A study of the separation efficiency in thermal diffusion column with a vertical permeable barrier. *AIChE Journal*, *32*, 971.

Figure Legends

Fig. 1. Parallel-plate membrane extractor with concurrent-flow operation and countercurrent-flow reflux.

Fig. 2. Parallel-plate membrane extractor with countercurrent-flow operation and concurrent-flow reflux.

Fig. 3. Mass-transfer rate obtained in the device of concurrent-flow operation with countercurrent-flow reflux.

Fig. 4. Mass-transfer rate obtained in the device of countercurrent-flow operation with concurrent-flow reflux.

Fig. 5. Comparison of W obtained under cocurrent-flow operation for R=1 and Δ=0.1 ~ 0.5 with that for Δ=0.5 and R = 2 and 3.

Fig. 6. Comparison of W obtained under cocurrent-flow operation for R=2 and Δ=0.1 ~ 0.5 with that for Δ=0.5 and R = 3 ~ 5.

Fig. 7 Comparison of W obtained under countercurrent-flow operation for R=1 and Δ=0.5 ~ 0.9 with that for Δ=0.5 and R = 2 ~ 8.

Fig. 8. Comparison of W obtained under countercurrent-flow operation for R=2 and Δ= 0.5 ~ 0.9 with that for Δ=0.5 and R = 3 ~ 8.

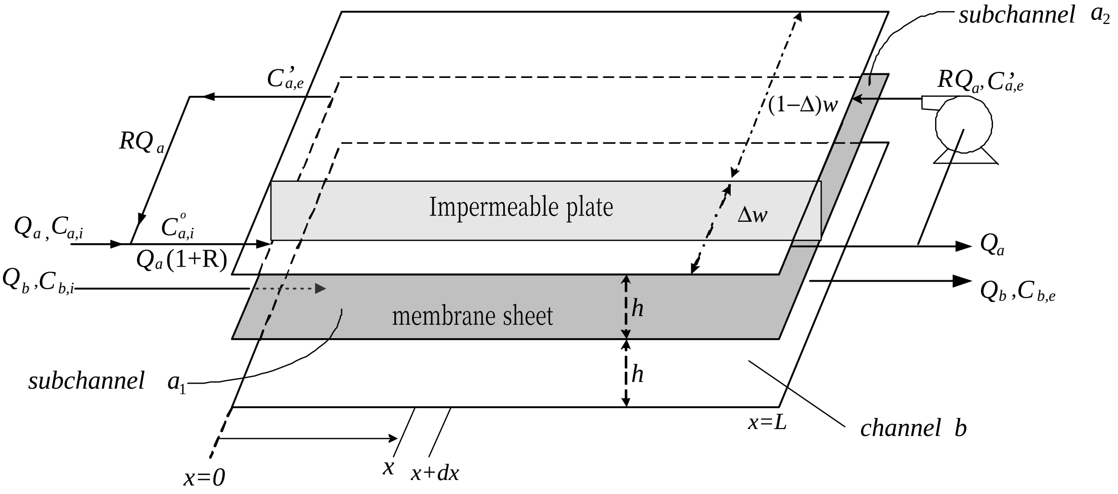

(a) Schematic diagram

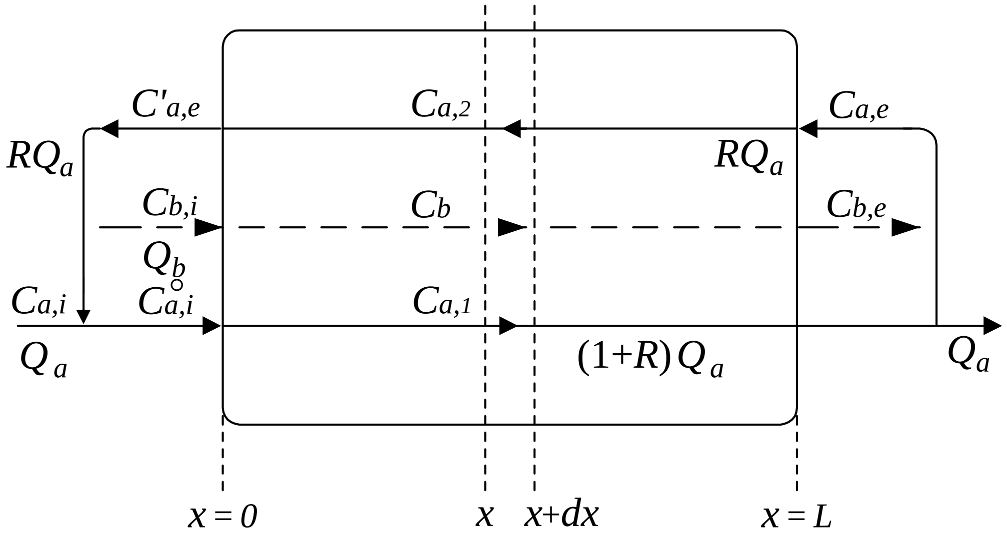

(b) Flow chart

Fig. 1

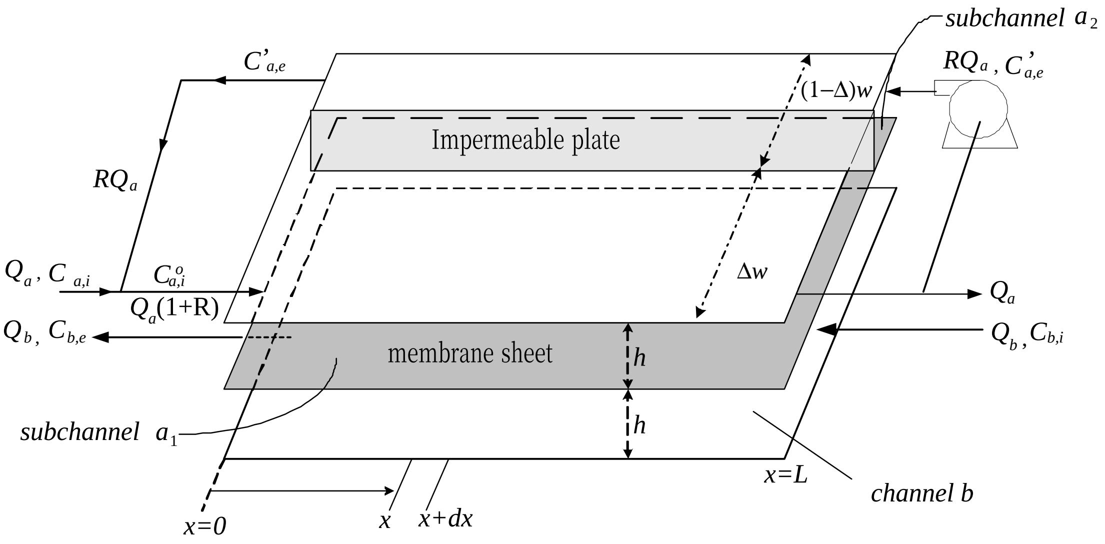

(a) Schematic diagram

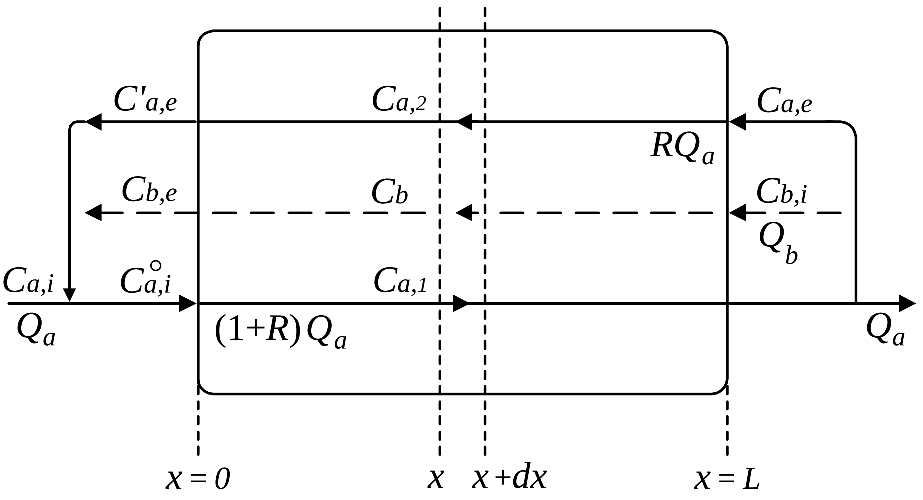

(b) Flow chart

Fig. 2

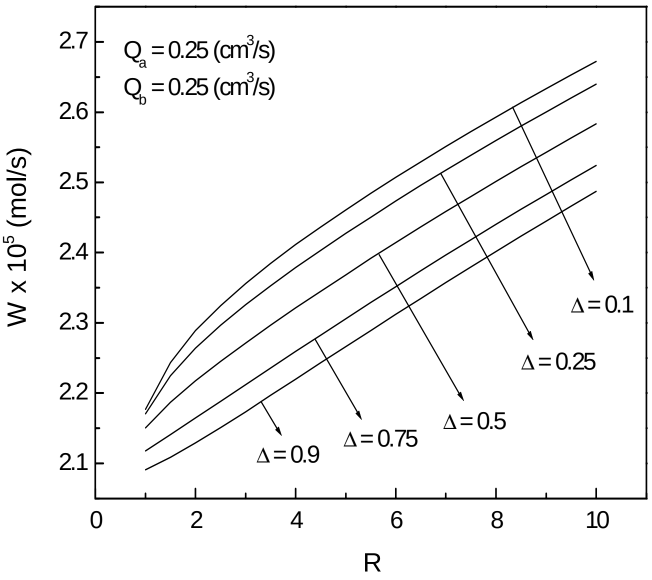

(a) $C_{a,i} = 0.5 \times 10^{-3} mole / cm^3$

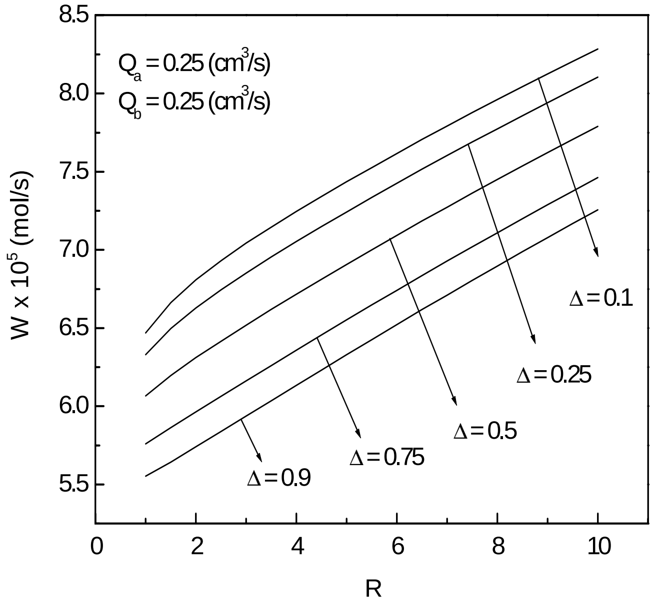

(b) $C_{a,i} = 2.0 \times 10^{-3} mole / cm^3$

Fig. 3

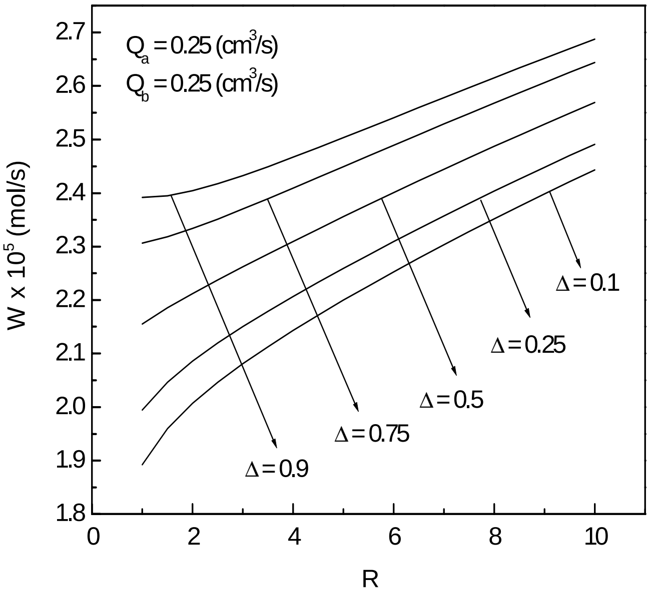

(a) $C_{a,i} = 0.5 \times 10^{-3} mole/cm^3$

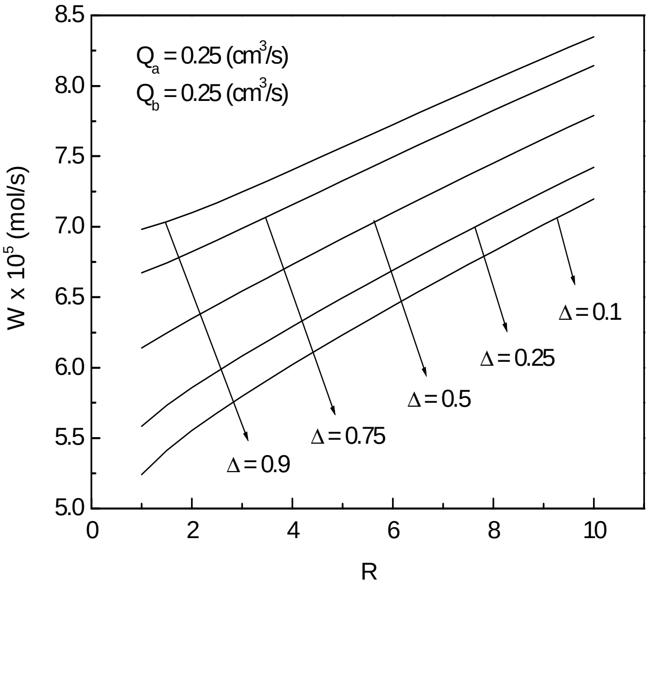

(b) $C_{a,i} = 2.0 \times 10^{-3} mole/cm^3$

Fig. 4

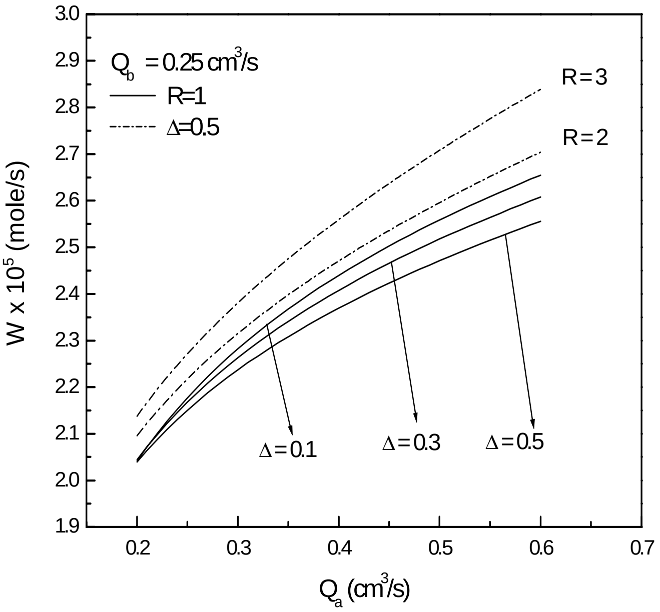

(a) $C_{a,i} = 0.5 \times 10^{-3}\ mole/cm^3$

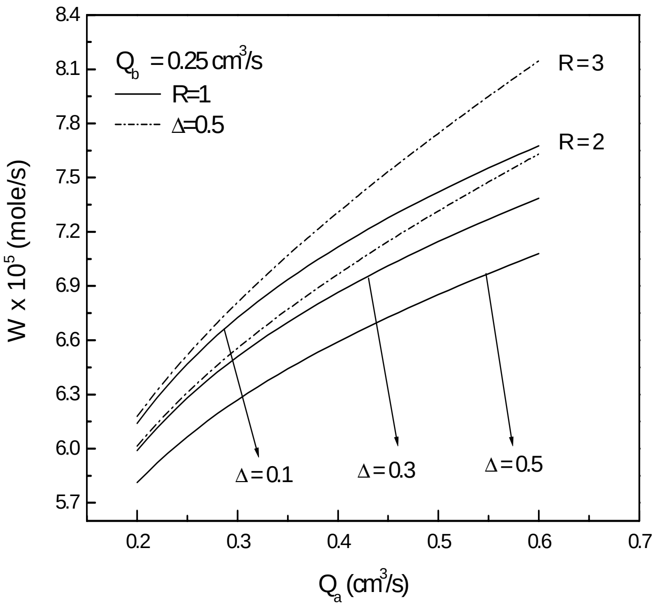

(b) $C_{a,i} = 2.0 \times 10^{-3}\ mole/cm^3$

Fig. 5

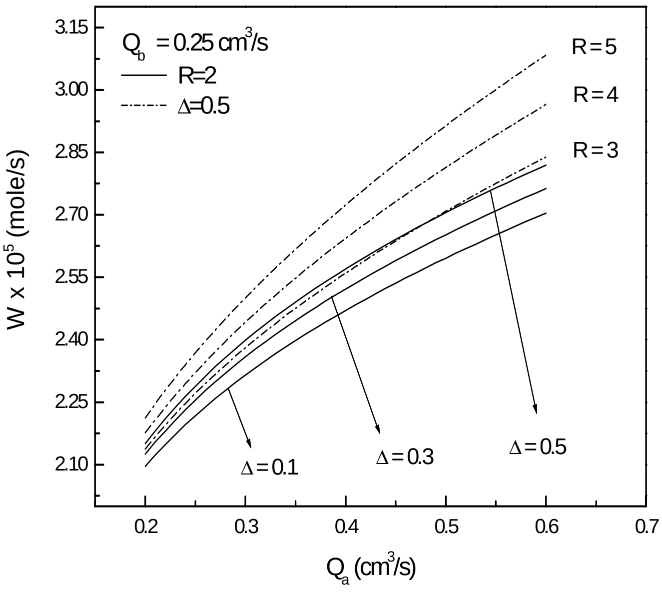

(a) $C_{a,i} = 0.5 \times 10^{-3}\, mole / cm^3$

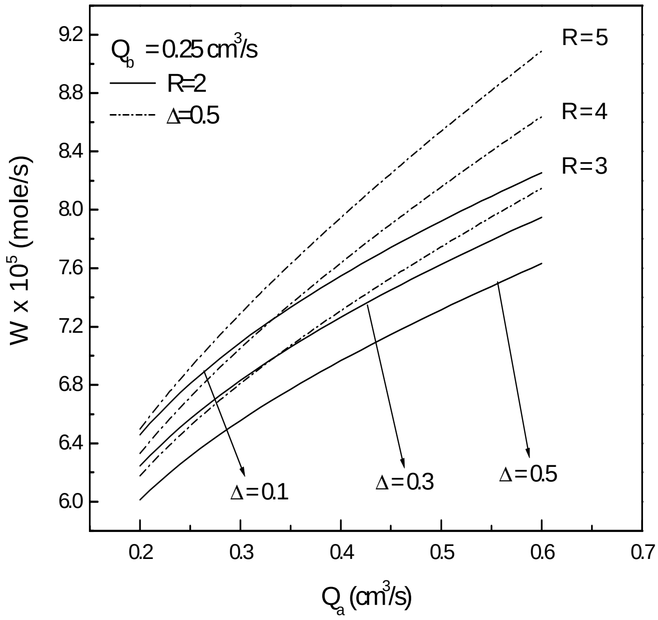

(b) $C_{a,i} = 2.0 \times 10^{-3}\, mole / cm^3$

Fig. 6

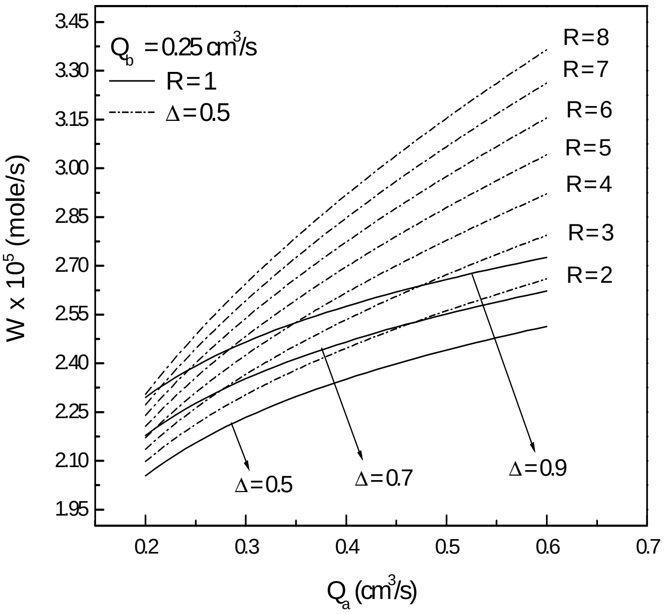

(a) $C_{a,i} = 0.5 \times 10^{-3}\ mole/cm^3$

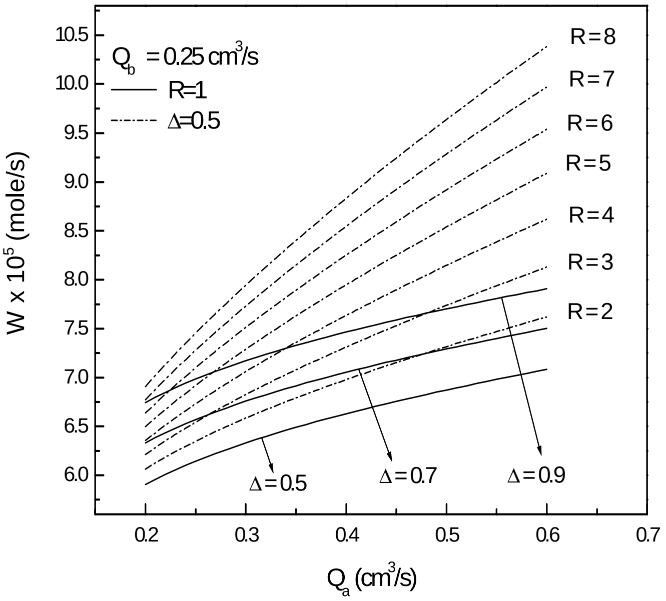

(b) $C_{a,i} = 2.0 \times 10^{-3}\ mole/cm^3$

Fig. 7

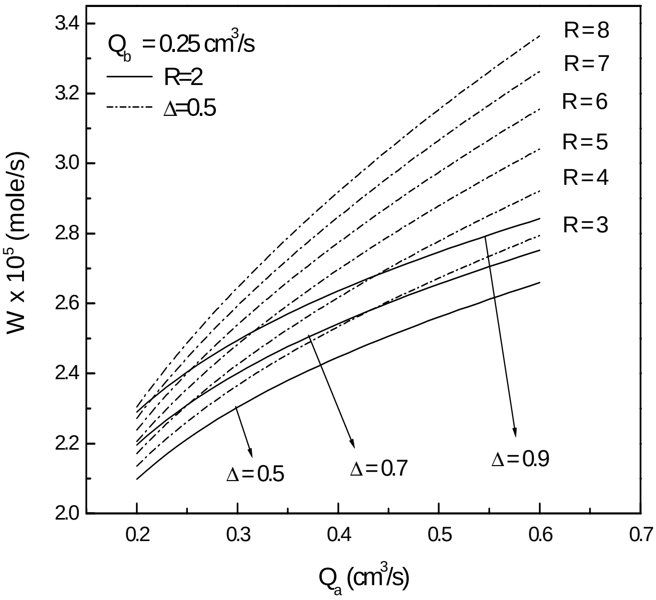

(a) $C_{a,i} = 0.5 \times 10^{-3}\, mole / cm^3$

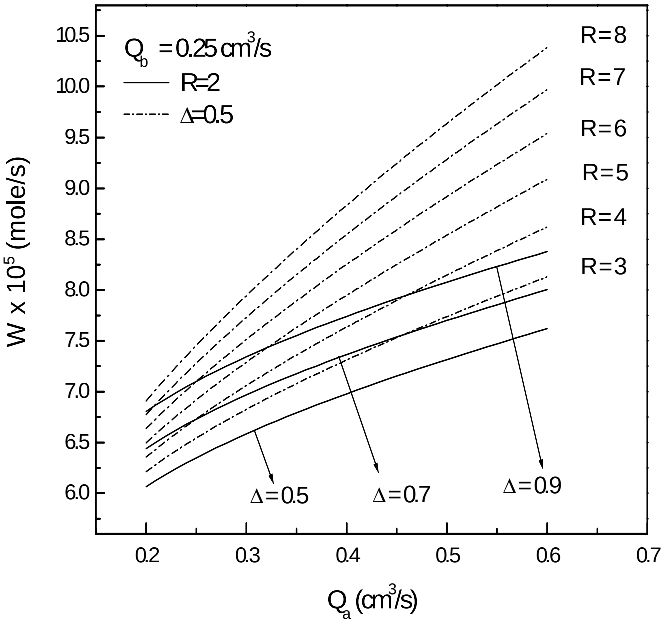

(b) $C_{a,i} = 2.0 \times 10^{-3}\, mole / cm^3$

Fig. 8

Table 1

Predicting results of concurrent-flow operation with countercurrent-flow reflux : $C_{a,i} = 2.02\times10^{-3} mole/cm^3$, $Q_b = 0.25 cm^3/s$ and $C_{b,i} = 0$

Q_a (cm^3/s)	R	$W\times10^5$ (mole/s)	I (%)				H × 10^9 (hp)				
		Δ=0.5	Δ=0.1	Δ=0.25	Δ=0.75	Δ=0.9	Δ=0.1	Δ=0.25	Δ=0.5	Δ=0.75	Δ=0.9
0.2	0.5	5.6276	1.80	1.52	-3.03	-5.68	1.20	0.50	0.27	0.22	0.27
0.2	1	5.8112	5.66	3.76	-4.57	-7.76	2.16	0.92	0.53	0.50	0.77
0.2	5	6.4799	7.64	4.86	-5.18	-8.45	20.25	9.27	6.38	7.74	15.15
0.2	9	7.0338	6.83	4.34	-4.58	-7.45	56.89	26.52	18.90	23.88	48.08
0.4	0.5	6.3518	6.18	4.12	-5.05	-8.59	4.77	1.96	1.06	0.85	1.06
0.4	1	6.5919	7.97	5.12	-5.66	-9.34	8.59	3.63	2.10	1.96	3.03
0.4	5	7.9527	7.19	4.55	-4.76	-7.73	80.96	37.03	25.48	30.91	60.55
0.4	9	9.1207	5.69	3.60	-3.75	-6.07	227.54	106.05	75.58	95.48	192.28
0.6	0.5	6.7591	7.55	4.91	-5.60	-9.33	10.71	4.40	2.36	1.89	2.36
0.6	1	7.0786	8.44	5.39	-5.80	-9.49	19.32	8.15	4.71	4.40	6.80
0.6	5	9.1091	6.35	4.01	-4.17	-6.75	182.14	83.30	57.31	69.52	136.21
0.6	9	10.8066	4.62	2.92	-3.02	-4.89	511.95	238.60	170.03	214.80	432.62
0.8	0.5	7.0731	8.08	5.2	-5.76	-9.50	19.03	7.80	4.19	3.35	4.19
0.8	1	7.4781	8.44	5.37	-5.71	-9.31	34.34	14.48	8.36	7.80	12.07
0.8	5	10.1365	5.57	3.52	-3.65	-5.90	323.79	148.08	101.88	123.59	242.15
0.8	9	12.2793	3.79	2.40	-2.48	-4.00	910.12	424.17	302.27	381.87	769.10

Table 2

Predicting results of countercurrent -flow operation with concurrent -flow reflux : $C_{a,i} = 2.02\times10^{-3} mole/cm^3$, $Q_b = 0.25cm^3/s$ and $C_{b,i} = 0$

Q_a (cm^3/s)	R	$W\times10^5$ (mole/s)	I (%)			
		Δ=0.5	Δ=0.1	Δ=0.25	Δ=0.75	Δ=0.9
0.2	0.5	5.7900	-18.87	-11.52	10.67	16.68
0.2	1	5.9052	-15.34	-9.45	9.01	14.21
0.2	5	6.4975	-10.31	-6.37	6.13	9.69
0.2	9	7.0403	-8.51	-5.25	5.04	7.97
0.4	0.5	6.4283	-15.66	-9.62	9.08	14.28
0.4	1	6.6284	-13.00	-8.28	7.97	12.61
0.4	5	7.9469	-8.73	-5.40	5.23	8.29
0.4	9	9.1101	-6.63	-4.10	3.97	6.29
0.6	0.5	6.7913	-14.18	-8.73	8.31	13.09
0.6	1	7.0833	-12.29	-7.60	7.34	11.63
0.6	5	9.0875	-7.45	-4.61	4.47	7.09
0.6	9	10.7845	-5.27	-3.26	3.16	5.02
0.8	0.5	7.0750	-13.20	-8.14	7.78	12.29
0.8	1	7.4596	-11.46	-7.09	6.86	10.87
0.8	5	10.1025	-6.43	-3.98	3.87	6.13
0.8	9	12.2485	-4.29	-2.66	2.58	4.09